

Deep learning directed synthesis of fluid ferroelectric materials

Charles Parton-Barr¹, Stuart R. Berrow¹, Calum J. Gibb², Jordan Hobbs¹, Wanhe Jiang¹, Caitlin O'Brien^{2,3}, Will C. Ogle^{2,3}, Helen F. Gleeson¹, Richard J. Mandle^{1,2,*}

¹School of Physics and Astronomy, University of Leeds, Leeds, UK, LS29JT

²School of Chemistry, University of Leeds, Leeds, UK, LS29JT

³School of Applied Mathematics, University of Leeds, Leeds, UK, LS29JT

* r.mandle@leeds.ac.uk

Abstract

Fluid ferroelectrics, a recently discovered class of liquid crystals that exhibit switchable, long-range polar order, offer opportunities in ultrafast electro-optic technologies, responsive soft matter, and next-generation energy materials. Yet their discovery has relied almost entirely on intuition and chance, limiting progress in the field. Here we develop and experimentally validate a deep-learning data-to-molecule pipeline that enables the targeted design and synthesis of new organic fluid ferroelectrics. We curate a comprehensive dataset of all known longitudinally polar liquid-crystal materials and train graph neural networks that predict ferroelectric behaviour with up to 95% accuracy and achieve root mean square errors as low as 11 K for transition temperatures. A graph variational autoencoder generates de novo molecular structures which are filtered using an ensemble of high-performing classifiers and regressors to identify candidates with predicted ferroelectric nematic behaviour and accessible transition temperatures. Integration with a computational retrosynthesis engine and a digitised chemical inventory further narrows the design space to a synthesis-ready longlist. 11 candidates were synthesised and characterized through established mixture-based extrapolation methods. From which extrapolated ferroelectric nematic transitions were compared against neural network predictions. The experimental verification of novel materials augments the original dataset with quality feedback data thus aiding future research. These results demonstrate a practical, closed-loop approach to discovering synthesizable fluid ferroelectrics, marking a step toward autonomous design of functional soft materials.

Introduction

The design of molecular materials requires domain specific expertise and understanding of the complex, often multidimensional relationship between chemical structure and macroscopic properties [1]. The vastness of chemical space means that discovering new molecular materials through exploratory synthesis is inherently slow [2]. It requires significant experimental effort to iteratively expand from known structures, a process prone to the encoding of human bias. Advances in computational power and algorithmic efficiency make deep learning an ever more practical approach for extracting structure-property relationships from large molecular datasets [3]. Coupled to generative models capable of designing new molecular structures [4], this enables the data-driven exploration of chemical space and opens a new paradigm in the design of molecular materials. The end point of molecule design is their physical realisation. To best achieve this, the generative workflow output must be guided by a set of requirements [5]. The molecules need to be realistically synthesisable, property prediction must be rigorously justified, expert human feedback integrated, and analysis of predictions should elucidate structural property relations.

Approaches for generating novel molecules can be broadly classified into rule-based systems and generative machine-learning models. Rule-based approaches construct new molecules by recombining predefined structural fragments or applying encoded chemical reactions [6]. In contrast, generative models learn a latent representation of chemical space from training data, sampling this latent space to propose new chemical structures [7]. Deep generative models have been developed using recurrent neural networks [8], variational autoencoders [9], and generative adversarial networks; [10] each learning the implicit molecular syntax (e.g. from SMILES strings) and producing novel candidate structures. Recently, molecular graph neural networks have been combined with variational autoencoder architectures to generate new graph structures [11]. While these methods have been successfully and widely applied in the context of drug discovery [12], protein structure [13], and inorganic/solid-state materials [14], they are yet to significantly impact the design of soft materials [15].

Liquid crystals provide a demanding testbed for molecular design: their bulk properties emerge from molecular structure through subtle and collective interactions that are not captured by simple molecular descriptors. Liquid crystals are soft phases of matter that combine degrees of orientational and positional order with fluidity, giving rise to states of matter (mesophases) with distinct symmetry and physical properties [16-18]. Amongst these phases is the recently discovered ferroelectric nematic (N_F) phase (Fig. 1a) which long range polar order arising from the parallel arrangement of molecular dipoles yields bulk spontaneous polarisation comparable to solid state ferroelectrics [19]. This can be compared to a conventional nematic phase in which the nematic phase's inversion symmetry of its dipole moments is broken.

The formation of liquid crystal phases and their specific mesophase type depends on a delicate balance of molecular shape and electronic structure, which impact on collective molecular organisation. Small structural modifications can give rise to significant differences in phase behaviour, making traditional structure-property heuristics unreliable. Only a small number of structural motifs are currently known to support the N_F phase, notably DIO [20], RM734 [21, 22] (Fig. 1b) and derivatives thereof [23-26]. This narrow chemical space stems from an absence of design rules for the structural-property relationship that causes the spontaneous polarity to emerge [27-30]. Identifying new structural motifs capable of stabilising polar order therefore presents a significant challenge in the molecular design of such materials.

Machine learning studies in liquid crystal science have focused on property prediction or classification rather than molecular design. Examples include models for the classification of ferroelectric nematic materials [31], predicting clearing point (isotropisation) temperatures [32, 33], phase transitions in bent-core type materials [34], lyotropic phase behaviour [35], image-based frameworks for phase identification via optical texture analysis [36, 37], hydrodynamic properties via director field dynamics [38], and optimisation of LCD backlight technology [39]. Each of these studies illustrates the promise of data-driven methods in liquid crystal research but none address generative molecular design with explicit synthesis of new materials, which is the focus of the present work.

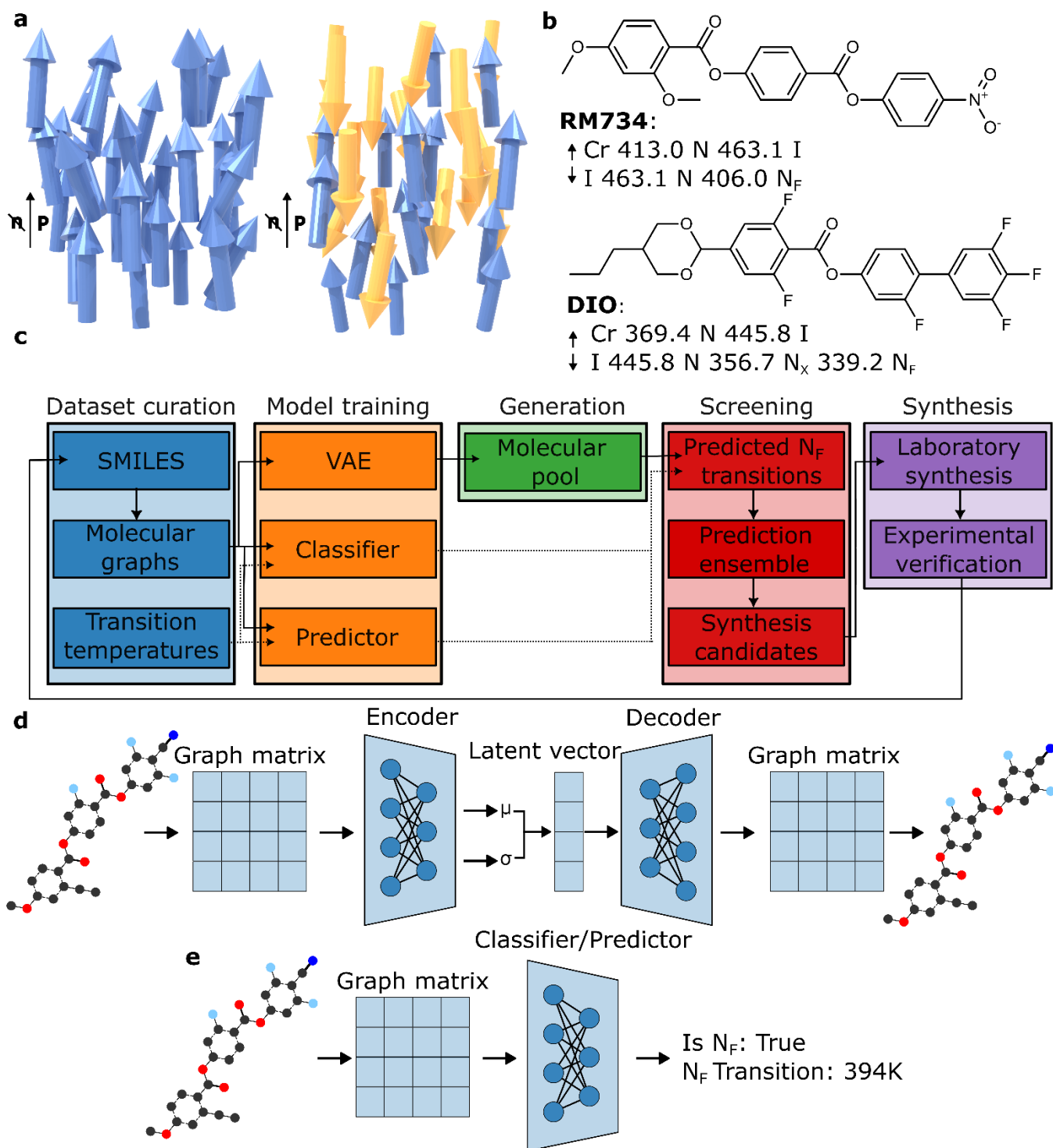


Figure 1. a) A schematic representation of the ferroelectric nematic (N_F) phase (right), in which molecular dipoles align collectively to produce macroscopic polar order and lack inversion symmetry. (b) Representative N_F materials RM734 and DIO, with molecular structures, transition temperatures in K. (c) Overview of the generative–predictive workflow for data-driven discovery of N_F materials, including dataset curation, model training, molecular generation, screening, and experimental validation. (d) Variational autoencoder architecture used for molecular generation. (e) Neural-network classifier and property prediction model architectures.

Here we introduce a generative-predictive framework for small-molecule design and apply it to the discovery of new ferroelectric nematic materials. This workflow (Fig. 1c) generates candidate structures and predicts N_F behaviour and transition temperatures, providing a data-driven approach to exploring the chemical space associated with this state of matter. We validate the framework by synthesis and characterisation of model-generated candidates; these form an *ex-silico* testing set, its investigation of the N_F chemical space providing valuable feedback for further training of machine learning of models. The complete workflow establishes an experimental benchmark for data-driven materials discovery. The complete set of synthesised candidates with extrapolated transition temperatures can be found in the ESI.

Methods

Data setup

We curated a dataset comprising >500 small-molecule liquid crystal materials which includes all reported N_F materials, up to October 2025 and a further >200 materials from unpublished in-house measurements. Each entry consists of the molecular structure as SMILES and experimentally measured phase transition temperatures. To avoid biasing the model towards N_F behaviour the dataset was balanced with structurally similar non- N_F materials

Model training

Smiles strings were converted to molecular graphs using RDKit. In the graph representation, each molecule is represented by a node feature matrix, V (atom descriptors) and an edge matrix, E (bond connectivity). These graph representations were annotated with transition temperatures and used as inputs for deep-learning models (Fig. 1(d,e)).

We employ three neural architectures: (a) a graph variational autoencoder (VAE) for generation of *de novo* structures (b) a binary classifier to predict the presence or absence of N_F behaviour; (c) a scalar predictor (regression model) for predicting N_F transition temperatures (Fig. 1e).

The VAE is a modified MGVAE architecture [11] and learns a probabilistic latent representation of molecular structure. The encoder maps molecular graphs into a continuous latent space, and the decoder reconstructs graphs from latent vectors (i.e. the inverse process), enabling the generation of novel molecules

For classification and regression graph neural networks transform molecular graphs in scalar outputs corresponding to phase assignment or N_F transition temperature. Our work includes a library of architectures comprising GATCONV [40], GATv2CONV [41], GINCONV [42], GCNCONV [43], GatedGraphConv [44], TransformerConv[45].

Given the modest size of our dataset (~700 molecules) repeated k-fold cross-validation was used for model training and performance evaluation. Hyperparameter settings for the training of models can be found in the supplementary information.

Generation

After training the VAE model was used to generate novel molecular structures by sampling its latent space and decoding the resulting vectors into molecular graphs. Because the latent space derives from experimentally characterised liquid crystal molecules, the generated structures occupy a similar chemical manifold (“dataset-like”) while also allowing exploration of chemical space beyond the training set

The decoded molecular graphs were converted into canonical SMILES strings; after filtering any duplicates this yields a pool of novel molecules occupying the learned N_F liquid crystal chemical manifold, 15413 novel structures overall.

Screening

We construct an ensemble of classifiers by selecting the three most accurate models (Fig. 2a) from across four different graph neural network architectures. Each classifier simply returns a Boolean value indicating the presence or absence of the N_F phase. An analogous ensemble of predictors (Fig. 2b) was selected in the same manner, choosing for the lowest root mean square error (RMSE) of N_F transition temperature predictions.

Molecules for which the ensemble of classifiers demonstrated high consensus were subsequently evaluated using the ensemble of predictors, with the mean predicted N_F transition temperature as a ranking criterion. This yields the generated pool of materials

From the screened pool we selected candidate molecules representing both high predicted likelihood of N_F behaviour and low-probability negative controls. Computational retrosynthesis tools [46] allied to our digitised chemical inventory and vendor catalogues allowed us to identify longlist of synthetically accessible targets. This machine generated longlist was then reviewed and prioritised by a team of human synthetic chemists

Synthesis

All compounds were synthesised using standard organic chemistry techniques in conventional laboratory glassware, either open to air or under an atmosphere of dry nitrogen. All chemical reactions were ultimately subject to purification by flash chromatography over silica gel using a Combiflash NextGen 300+ system (Teledyne Isco) with an appropriate solvent gradient. Final materials were filtered through 0.2-micron PTFE filters to remove particulates. Yields refer to isolated, spectroscopically homogenous material. Chemical characterisation was made by NMR spectroscopy (^1H , ^{13}C and ^{19}F) and high-resolution mass spectrometry (HRMS), all materials were confirmed to have purity of >99% (peak area) by reverse phase HPLC. Full synthetic details are given in the ESI to this article. Synthesised materials were studied by polarised optical microscopy (POM) and differential scanning calorimetry (DSC). Transition temperatures for polar phases were extrapolated from mixture studies with DIO as the host (~90 wt%) and the material in question as the guest (~10 wt%).

Results

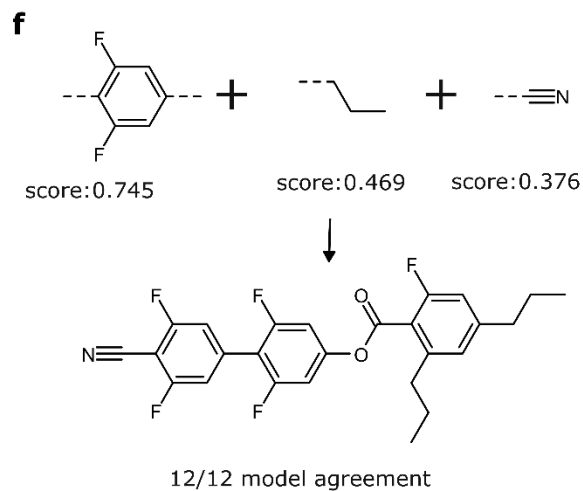
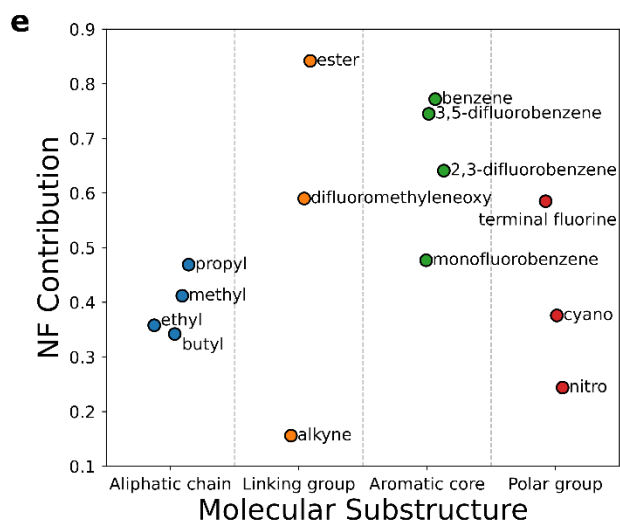
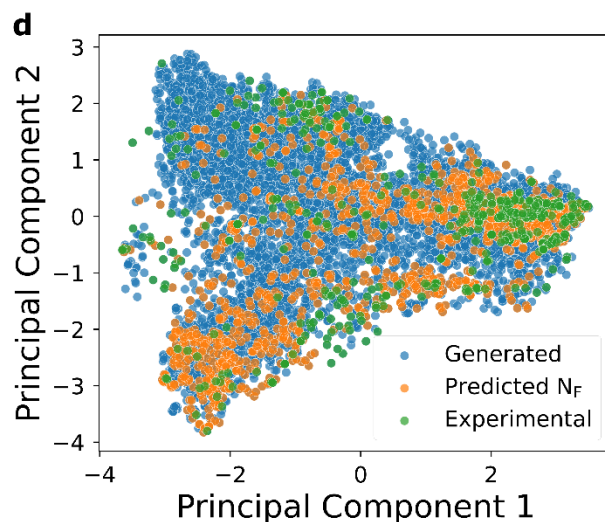
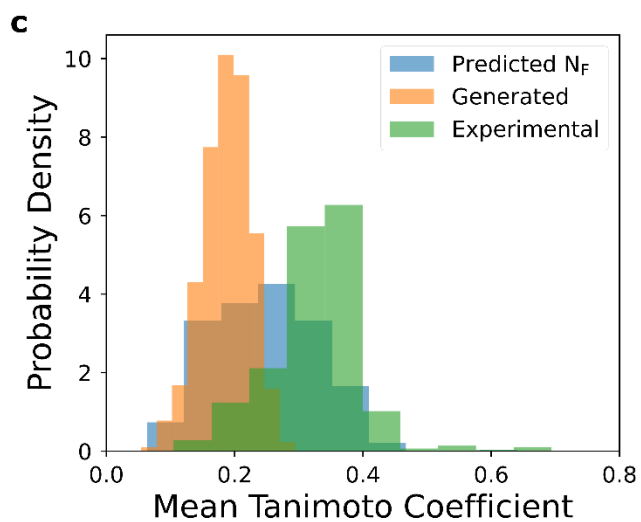
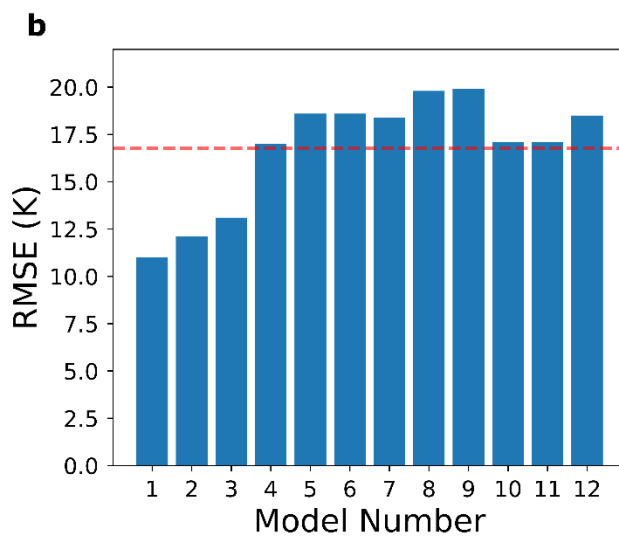
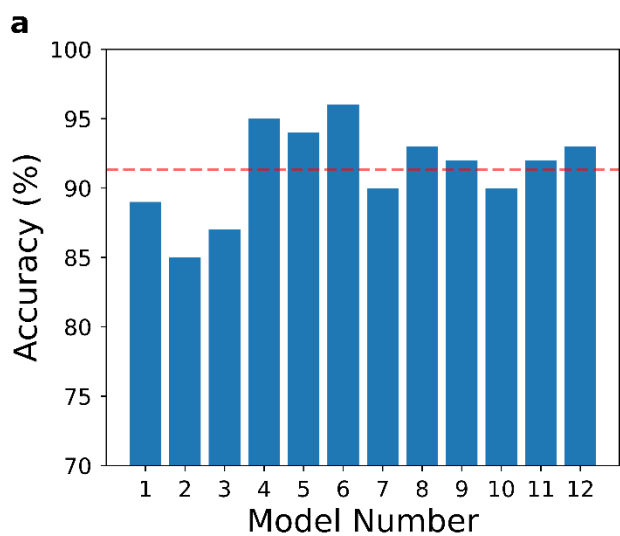


Figure 2. Analysing the model decisions in classifying a material as N_F . The a) accuracy and b) RMSE of a selected ensemble of models with the dashed line indicating the mean value. c) The Tanimoto coefficients comparing the molecule similarity within the three datasets. d) Visualisation of the structural similarity of the total three datasets. e) subgraph masking explanation scoring of the contribution to the N_F phase for molecular substructures present in the generated molecules. f) contribution-guided design coupled with scaffold analysis of the dataset.

To evaluate how the generative model explores chemical space relative to the experimental dataset, we compared distributions of selected structural descriptors (Fig. S10). The generated molecules exhibit broader variability in size and ring count, while retaining similar overall carbon distributions. Nitrogen-containing structures are less common in the generated set, whereas fluorination increases modestly. Oxygen counts shift toward simpler structures, suggesting the model samples lower-polarity motifs while retaining ester functionality. Substructure analysis (SMARTS-based) indicates reduced frequency of specific motifs that are over-represented in the training set (e.g., multiple difluorobenzene rings), alongside emergence of new functionalities such as ketones. Collectively, these patterns indicate that the generative model learns the dominant structural trends in liquid-crystal materials while exploring adjacent chemical space rather than memorising training examples

Our classifier and predictor models comprise four different types of graph convolutional layers and we identify the most accurate models for each architecture via hyperparameter searching (Table S2). Evaluating the performance of trained models, all classifiers achieve accuracies above 80% with the best models (3-6, Fig. 2a) achieving >90%. Regression models for N_F transition temperatures exhibited RMSE values of 10-20 K, with the three lowest-error models based on GCN layers (1-3, Fig. 2b).

To assess whether the model explores new chemical space, we compared molecular similarity distributions across the experimental dataset, the generated pool, and the predicted N_F subset using Tanimoto coefficients of Morgan fingerprints (Fig. 2c). As expected, generated structures are more diverse than the experimental set, while predicted N_F candidates cluster closer to experimental N_F molecules, indicating that the model prioritises plausible N_F like scaffolds while expanding chemical diversity beyond known motifs

Principal component analysis (PCA) of molecular fingerprints further shows that generated and predicted N_F molecules populate regions adjacent to (but extending beyond) the experimentally explored N_F space (Fig. 2d), confirming that the generative model proposes novel yet chemically realistic structures.

To gain insight into model decisions, we applied the substructure-masking explanation method (SME) [47] to quantify the influence of functional groups on N_F predictions (Fig. 2e). Removing specific fragments and recomputing predictions yields a per-fragment contribution score, identifying structural features that promote or suppress N_F behaviour. Combining high-contribution motifs provides a rational, interpretable route to designing candidate molecules (Fig. 2f), complementing chemical intuition.

Test set validation

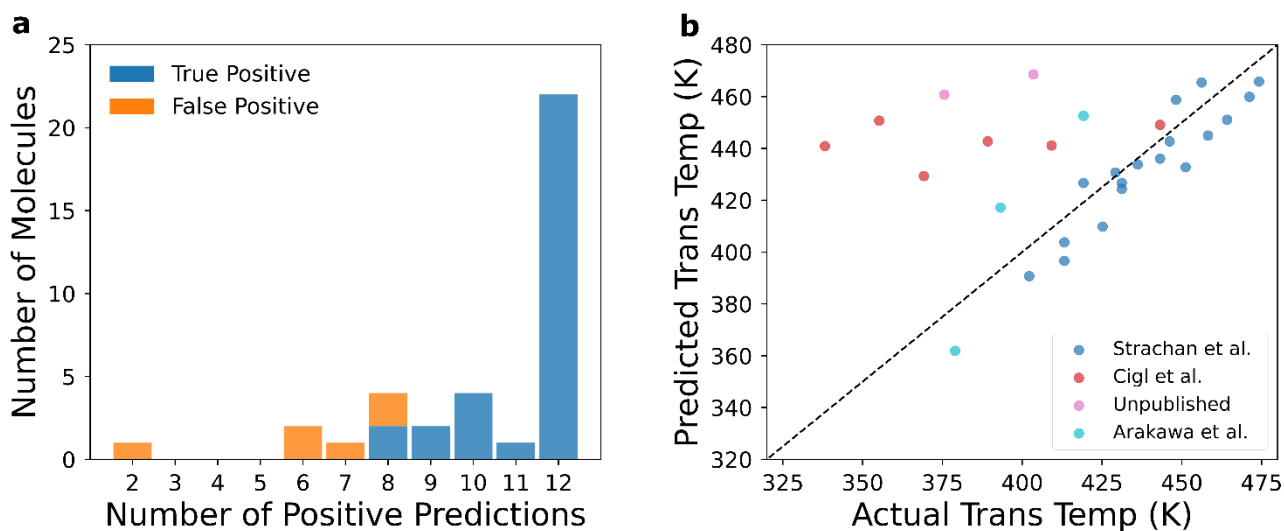


Figure 3. Test set evaluation of models. A) The distribution of positive predictions a molecule receives and how that relates to its NF phase ground truth label. B) Predicted vs actual N_F transition temperatures

To evaluate generalization performance, the classifier and regression ensembles were applied to an external test set of 39 molecules which were reported in the literature after the completion of model training [48-50]. As shown in Fig. 3a, molecules receiving high classifier consensus ($\geq 9/12$ positive votes) were all true N_F materials, whereas compounds predicted positive by ≤ 8 models included false positives. This demonstrates that ensemble agreement acts as a confidence metric and that a high consensus threshold improves precision when selecting synthesis candidates. Predicted vs actual N_F transition temperatures for the same test set (Fig. 3b) yielded an RMSE of ~ 25 K. Predictions are most accurate for molecules structurally similar to those in the training set, while larger deviations occur for out-of-distribution structures (such as those in Arakawa et al. which contain coumarin-type structures which are not featured in the training set at all). The performance of our models is consistent with expected behaviour for models trained on a finite chemical domain.

Synthesis and experimental validation of *de novo* compounds

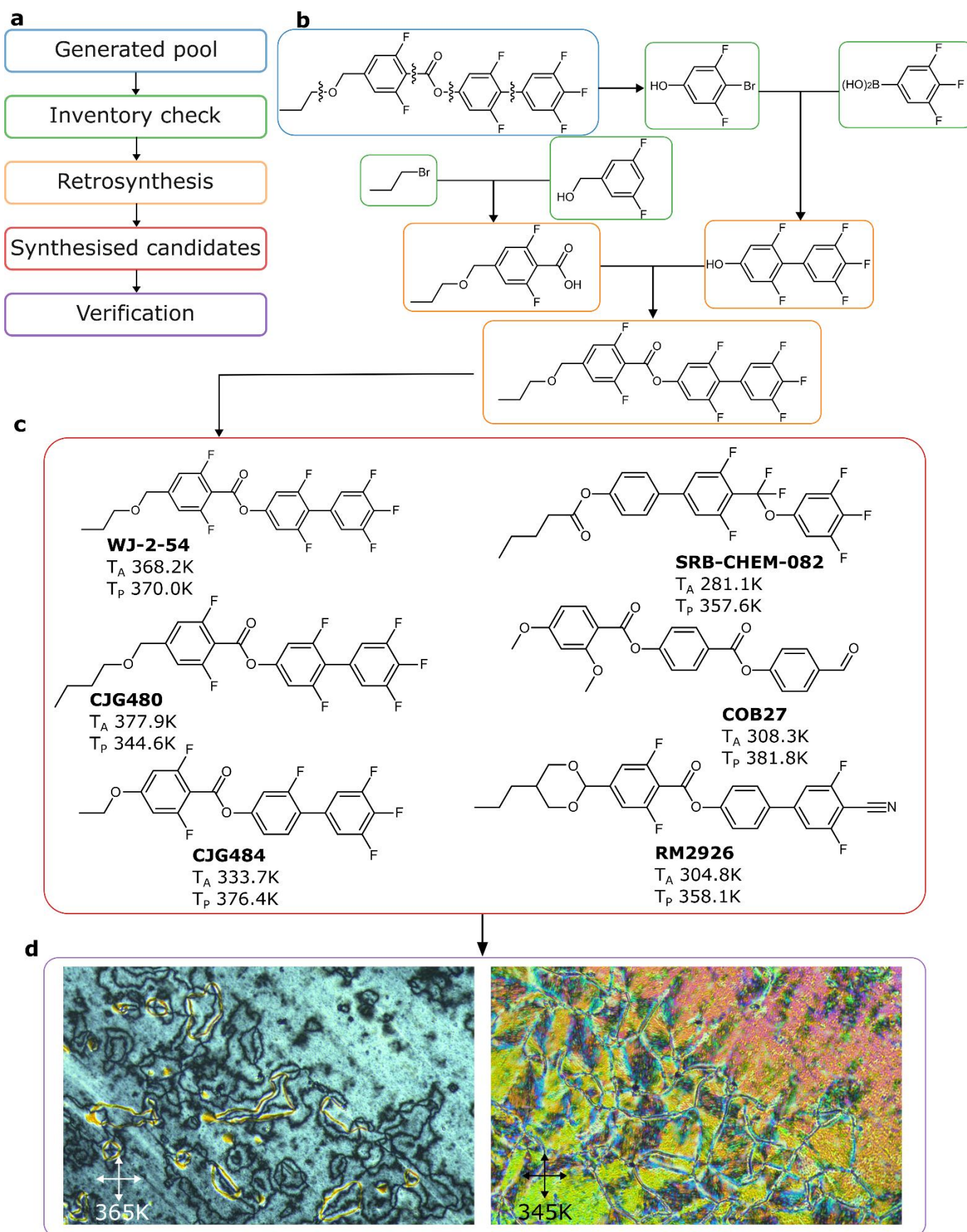


Figure 4. From machine learning predictions to experimental verification. A) The stages of the workflow that takes the molecules from generated to physical materials. b) Retrosynthesis coupled with a laboratory stock inventory assists in the identification of readily synthesisable molecules within the generated pool. c) Synthesised N_F structures and their extrapolated (T_A) and predicted (T_P) N_F transition temperatures. d) Once synthesized, POM analysis of 90wt% DIO: 10 wt% guest mixtures are used to extrapolate N_F transition temperatures

To select synthetically tractable targets from the generated pool we employed AiZynthFinder [46] to identify feasible retrosynthetic routes. The requires precursors were cross referenced with our in-house digitised chemical inventory (Fig. 4b), yielding a list of materials which could be rapidly accessible. Synthesis candidates were subsequently reviewed by synthetic chemists to confirm feasibility. From this process, we synthesised 11 previously unreported materials. All materials obtained in >99% purity (peak area) as judged by C18-HPLC analysis and were fully characterised; full synthetic details are given in the ESI to this article. The structures of a selection of these synthesised N_F candidates are given in figure 5d with their extrapolated actual transition temperatures (T_A ; K) and predicted transition temperatures (T_P ; K). The resulting dataset provides a direct test of the generative-predictive pipeline. The molecules can be assessed and used to augment the original experimental dataset, providing further structural data from which the models can learn from in further iterations of this process, thus continuing to guide molecular discovery. Molecules with a high chemical similarity to existing N_F materials (CJG480, CJG484, WJ- 2-54) have extrapolated N_F transition temperatures within 43K of the predicted values. There is a growth in error as the structures increasingly differ from experimental dataset culminating in a maximum error of 76K (SRB-CHEM-082). Full details of extrapolated N_F transitions for the complete set of synthesised molecules can be found in the supplementary information.

Conclusion

A generative-predictive framework for data-driven design and experimental validation of small molecules is presented. By integrating molecular graph learning, ensemble prediction, retrosynthetic filtering, and laboratory synthesis, this provides a practical end-to-end approach for accelerating materials discovery.

Applied to the discovery of ferroelectric nematic liquid crystals, we use this workflow to generate synthetically accessible candidates, from which we prepared several previously unreported compounds. Several possess extrapolated N_F transitions within reasonable boundaries, demonstrating that machine-learned chemical intuition can successfully guide molecular design in a domain where subtle structural changes govern emergent properties.

More broadly, this work illustrates a generalisable strategy for closed-loop molecular innovation: learn from experimental structure–property data, generate candidates within a realistic chemical manifold, triage using model consensus and retrosynthetic constraints, and validate in the laboratory. We expect this approach to extend to other classes of functional soft materials and to accelerate the rational exploration of chemical space.

Code and data availability

The code used in this article is available at <https://github.com/123cpb/nfml>. The data associated with this article is openly available from the University of Leeds Data Repository at <https://doi.org/10.5518/1798>

Author Contributions

The dataset was curated by CPB, JH, CJG, and RJM. CPB and RJM developed the machine learning code used in this work. Chemical synthesis was performed by SRB, COB, CJG, WJ, WCO, RJM. Characterisation of liquid crystalline behaviour was undertaken by (SRB, CPB, CJG, JH, WJ, WCO, COB, RJM). RJM and HFG secured funding. The first draft was written by CPB and RJM, with contributions from all authors.

Acknowledgements

RJM thanks: UKRI for funding via a Future Leaders Fellowship (Grant no MR/W006391/1; CJG, JH); Merck Electronics for funding via the LAMP2 Project (WJ, COB) and discussions around materials, The University of Leeds for funding via a University Academic Fellowship and a PhD Studentship for CPB; The SOFI2 CDT for funding PhD studentships for WCO and COB.

HFG thanks: S.R.B and H.F.G acknowledge funding from the Engineering and Physical Sciences Research Council, grant number EP/V054724/1.

This work was undertaken on the Aire HPC system at the University of Leeds, UK

References

1. Whitesides, G.M. and R.F. Ismagilov, *Complexity in chemistry*. science, 1999. **284**(5411): p. 89-92.
2. Reymond, J.-L., *The chemical space project*. Accounts of chemical research, 2015. **48**(3): p. 722-730.
3. Butler, K.T., et al., *Machine learning for molecular and materials science*. Nature, 2018. **559**(7715): p. 547-555.
4. Sanchez-Lengeling, B. and A. Aspuru-Guzik, *Inverse molecular design using machine learning: Generative models for matter engineering*. Science, 2018. **361**(6400): p. 360-365.
5. van den Broek, R.L., et al., *In Search of Beautiful Molecules: A Perspective on Generative Modeling for Drug Design*. Journal of Chemical Information and Modeling, 2025. **65**(18): p. 9383-9397.
6. Hartenfeller, M., et al., *DOGS: reaction-driven de novo design of bioactive compounds*. PLoS computational biology, 2012. **8**(2): p. e1002380.
7. Tong, X., et al., *Generative models for de novo drug design*. Journal of Medicinal Chemistry, 2021. **64**(19): p. 14011-14027.
8. Segler, M.H., et al., *Generating focused molecule libraries for drug discovery with recurrent neural networks*. ACS central science, 2018. **4**(1): p. 120-131.
9. Blaschke, T., et al., *Application of generative autoencoder in de novo molecular design*. Molecular informatics, 2018. **37**(1-2): p. 1700123.
10. Putin, E., et al., *Reinforced adversarial neural computer for de novo molecular design*. Journal of chemical information and modeling, 2018. **58**(6): p. 1194-1204.
11. Lee, M. and K. Min, *MGCVAE: Multi-Objective Inverse Design via Molecular Graph Conditional Variational Autoencoder*. Journal of Chemical Information and Modeling, 2022. **62**(12): p. 2943-2950.
12. Walters, W.P. and R. Barzilay, *Applications of deep learning in molecule generation and molecular property prediction*. Accounts of chemical research, 2020. **54**(2): p. 263-270.
13. Jumper, J., et al., *Highly accurate protein structure prediction with AlphaFold*. nature, 2021. **596**(7873): p. 583-589.
14. Xie, T. and J.C. Grossman, *Crystal graph convolutional neural networks for an accurate and interpretable prediction of material properties*. Physical review letters, 2018. **120**(14): p. 145301.
15. de Pablo, J.J., et al., *New frontiers for the materials genome initiative*. npj Computational Materials, 2019. **5**(1): p. 41.
16. Andrienko, D., *Introduction to liquid crystals*. Journal of Molecular Liquids, 2018. **267**: p. 520-541.
17. Chaikin, P.M. and T.C. Lubensky, *Principles of condensed matter physics*. 2000, Cambridge: Cambridge University Press.
18. Collings, P.J. and M. Hird, *Introduction to liquid crystals chemistry and physics*. The liquid crystals book series. 1997, London :: Taylor & Francis.
19. Sebastian, N., M. Copic, and A. Mertelj, *Ferroelectric nematic liquid-crystalline phases*. Physical Review E, 2022. **106**(2).
20. Nishikawa, H., et al., *A Fluid Liquid-Crystal Material with Highly Polar Order*. Advanced Materials, 2017. **29**(43).
21. Mandle, R.J., S.J. Cowling, and J.W. Goodby, *Rational Design of Rod-Like Liquid Crystals Exhibiting Two Nematic Phases*. Chemistry – A European Journal, 2017. **23**(58): p. 14554-14562.
22. Mandle, R.J., S.J. Cowling, and J.W. Goodby, *A nematic to nematic transformation exhibited by a rod-like liquid crystal*. Physical Chemistry Chemical Physics, 2017. **19**(18): p. 11429-11435.
23. Gibb, C.J., et al., *Spontaneous symmetry breaking in polar fluids*. Nature Communications, 2024. **15**(1): p. 5845.
24. Karcz, J., et al., *Spontaneous chiral symmetry breaking in polar fluid-helical ferroelectric nematic phase*. Science, 2024. **384**(6700): p. 1096-1099.

25. Hobbs, J., C.J. Gibb, and R.J. Mandle, *Ferri- and ferro-electric switching in spontaneously chiral polar liquid crystals*. Nature Communications, 2025. **16**(1): p. 7510.
26. Gibb, C.J., J. Hobbs, and R.J. Mandle, *Systematic Fluorination Is a Powerful Design Strategy toward Fluid Molecular Ferroelectrics*. Journal of the American Chemical Society, 2025. **147**(5): p. 4571-4577.
27. Osipov, M.A., *Dipole-dipole interactions and the origin of ferroelectric ordering in polar nematics*. Liquid Crystals, 2024. **51**(13-14): p. 2349-2355.
28. Hobbs, J., C.J. Gibb, and R.J. Mandle, *Polarity from the bottom up: a computational framework for predicting spontaneous polar order*. Journal of Materials Chemistry C, 2025. **13**(26): p. 13367-13375.
29. Cruickshank, E., *The Emergence of a Polar Nematic Phase: A Chemist's Insight into the Ferroelectric Nematic Phase*. ChemPlusChem, 2024. **89**(5): p. e202300726.
30. Madhusudana, N.V., *Simple molecular model for ferroelectric nematic liquid crystals exhibited by small rodlike mesogens*. Physical Review E, 2021. **104**(1): p. 014704.
31. Palacio-Betancur, V. and N.E. Jackson, *Molecular Charge Topologies Govern Polar Nematic Ordering*. Journal of the American Chemical Society, 2025.
32. Kränz, H., V. Vill, and B. Meyer, *Prediction of material properties from chemical structures. The clearing temperature of nematic liquid crystals derived from their chemical structures by artificial neural Networks*. Journal of chemical information and computer sciences, 1996. **36**(6): p. 1173-1177.
33. Johnson, S.R. and P.C. Jurs, *Prediction of the clearing temperatures of a series of liquid crystals from molecular structure*. Chemistry of materials, 1999. **11**(4): p. 1007-1023.
34. Antanasijević, D., et al., *A GMDH-type neural network with multi-filter feature selection for the prediction of transition temperatures of bent-core liquid crystals*. Rsc Advances, 2016. **6**(102): p. 99676-99684.
35. Le, T.C., et al., *Computational modeling and prediction of the complex time-dependent phase behavior of lyotropic liquid crystals under in meso crystallization conditions*. Crystal growth & design, 2013. **13**(3): p. 1267-1276.
36. Sigaki, H.Y., et al., *Estimating physical properties from liquid crystal textures via machine learning and complexity-entropy methods*. Physical Review E, 2019. **99**(1): p. 013311.
37. Pessa, A.A.B., et al., *Determining liquid crystal properties with ordinal networks and machine learning*. Chaos, Solitons & Fractals, 2022. **154**: p. 111607.
38. Zhou, Z., et al., *Machine learning forecasting of active nematics*. Soft matter, 2021. **17**(3): p. 738-747.
39. Mantel, C., et al., *Modeling the quality of videos displayed with local dimming backlight at different peak white and ambient light levels*. IEEE Transactions on Image Processing, 2016. **25**(8): p. 3751-3761.
40. Veličković, P., et al., *Graph attention networks*. arXiv preprint arXiv:1710.10903, 2017.
41. Brody, S., U. Alon, and E. Yahav, *How attentive are graph attention networks?* arXiv preprint arXiv:2105.14491, 2021.
42. Xu, K., et al., *How powerful are graph neural networks?* arXiv preprint arXiv:1810.00826, 2018.
43. Kipf, T., *Semi-supervised classification with graph convolutional networks*. arXiv preprint arXiv:1609.02907, 2016.
44. Li, Y., et al., *Gated graph sequence neural networks*. arXiv preprint arXiv:1511.05493, 2015.
45. Shi, Y., et al., *Masked label prediction: Unified message passing model for semi-supervised classification*. arXiv preprint arXiv:2009.03509, 2020.
46. Genheden, S., et al., *AiZynthFinder: a fast, robust and flexible open-source software for retrosynthetic planning*. Journal of Cheminformatics, 2020. **12**(1): p. 70.
47. Wu, Z., et al., *Chemistry-intuitive explanation of graph neural networks for molecular property prediction with substructure masking*. Nature Communications, 2023. **14**(1): p. 2585.
48. Strachan, G.J., E. Górecka, and D. Pocięcha, *Competition between mirror symmetry breaking and translation symmetry breaking in ferroelectric liquid crystals with increasing lateral substitution*. Materials Horizons, 2025.
49. Cigl, M., et al., *Giant permittivity in dimethylamino-terminated ferroelectric nematogens*. Journal of Molecular Liquids, 2023. **385**: p. 122360.
50. Arakawa, Y., et al., *Coumarin-based ferroelectric nematic liquid crystals*. Chemical Communications, 2025.